

Influence of Surface Halogenation on Silane Adsorption onto Si(001) Surface for Poly-Si Epitaxy: A Density Functional Theory Study with Neural Network Potential

Hyunhak Jeong
Mechatronics Research
Samsung Electronics Co., Ltd.
Hwaseong-si, South Korea
h152.jeong@samsung.com

Byungjo Kim
Mechatronics Research
Samsung Electronics Co., Ltd.
Hwaseong-si, South Korea
bold.kim@samsung.com

Suyoung Yoo
Mechatronics Research
Samsung Electronics Co., Ltd.
Hwaseong-si, South Korea
suyoung.yoo@samsung.com

Sang Ki Nam
Mechatronics Research
Samsung Electronics Co., Ltd.
Hwaseong-si, South Korea
sangki.j.nam@samsung.com

Abstract— In this study, we conducted Density Functional Theory (DFT) simulations to investigate the impact of surface halogenation on the dissociative adsorption of SiH₄ on crystalline Si(001) surface. First, we examined the adsorption energetics of surface halogenation using chlorine (Cl₂) molecules. The dissociative adsorption of Cl₂ exhibited a high reactivity with the undercoordinated surfaces without barrier. Molecular Dynamics (MD) simulations using Neural Network Potentials (NNP) has been developed and adopted to study surface diffusion of adsorbed Cl atoms and the surface concentration of Cl on the Si(001) surface at higher temperature. Second, we conducted subsequent silane (SiH₄) adsorption and the first hydrogen dissociation on the bare and Cl-passivated surfaces. Our potential energy surface search revealed that the surface halogenation on the silicon surface suppresses the primary adsorption reaction of SiH₄. Overall, this study provides an atomistic description of the dissociative adsorption mechanisms and associated energies of Cl₂ and subsequent SiH₄ reactions for modeling the epitaxial deposition process and may serve as foundational knowledge for developing next-generation Si epitaxy techniques.

Keywords— *Density Functional Theory, Si epitaxy, Surface halogenation, Molecular dynamics, Neural network potential*

I. INTRODUCTION

Epitaxial growth of poly-Si using Chemical Vapor Deposition (CVD) is a widely used method for creating gate electrodes and hard mask layers in modern Complementary Metal Oxide Semiconductor (CMOS) technology. As device integrations consist of multiple repetitive combinations of individual manufacturing processes, the surface where the poly-Si will grow can exhibit a different surface termination depending on the prior process. This is crucial to understand the growth kinetics and their effect on the resulting poly-Si layer. For example, hydrogen termination on a Si(001) surface affects silane (SiH₄) adsorption energetics in comparison to undercoordinated surfaces, reducing activation energy for adsorption [1]. Additionally, as halogenated surfaces are frequently observed after etching of Si compounds, it is necessary to understand potential energy landscapes for primary adsorption reactions of SiH₄ chemistry that determine

the subsequent growth kinetics in order to elaborate the process. For this purpose, atomistic simulations could provide knowledge on the underlying mechanisms and kinetics [2]–[4]. Such knowledge may aid in opening a new window for better controllability in next-generation Si epitaxy techniques.

In this study, we conducted Density Functional Theory (DFT) simulations to investigate the impact of surface halogenation on the dissociative adsorption of SiH₄ on crystalline silicon surface: Si(001). First, we examined the adsorption energetics of surface halogenation using chlorine (Cl₂) molecules. The dissociative adsorption of Cl₂ exhibited a high reactivity with the undercoordinated surfaces. Molecular Dynamics (MD) simulations using Neural Network Potentials (NNP) has been developed and adopted to study surface diffusion of adsorbed Cl atoms and the surface concentration of Cl on the Si(001) surface at higher temperature. Second, we conducted subsequent silane (SiH₄) adsorption and the first hydrogen dissociation on the bare and Cl-passivated surfaces. Our potential energy surface search revealed that the surface halogenation on the silicon surface suppresses the initial adsorption reaction of SiH₄.

II. METHODS

A. Density Functional Theory Calculations

In this study, all the DFT calculations were performed using the Vienna ab initio simulation package (VASP) program with Perdew-Burke-Ernzerhof (PBE) functional under the projector-augmented wave method. Van der Waals corrections were imposed by the Grimme-D3 approach. The Kohn-Sham states were expressed within an optimal cutoff energy of 400 eV and the convergence criteria for the self-consistent field calculation were set to 1E-6 eV while the force criteria for structural relaxations were set to 0.02 eV/Å. Gaussian smearing method were used for the better convergence with $\sigma=0.05$ eV. For the surface modeling, we constructed Si(001)-(4×4) slab composed of seven atomic layers. The Brillouin zone was sampled in a (2×2×1) grid with the Monkhorst-Pack scheme. The clean top surface of the Si(001) slab exhibited the well-known buckled dimers with a c(4×2) superstructure. The calculated dimer tilt angle and

bond length between Si-Si were 18.9° , and 2.37 \AA , which are in good agreement with other simulation results, 18.6° , and 2.36 \AA , respectively [5]. Finally, the minimum energy paths of SiH_4 adsorption were determined using climbing image Nudged Elastic Band (cNEB) method [6].

B. Neural Network Potential Generation

In order to study the dynamics and chemical activities of the Cl adatoms on the Si surface including surface diffusion and desorption of Cl atoms on the Si surface, MD simulations were conducted using NNP. The overall training and generation of the potential were performed under the framework of SIMPLE-NN [7]. SIMPLE-NN uses the Behler–Parrinello (BP) type symmetry function as descriptors for the artificial neural network. Each atomic position is converted to the symmetry function G vectors which consist of 8 radial components and 18 angular components for each atomic type. Feed-forward neural network consists of 2 layers of 30 nodes and the nodes were fully connected. For the training sets, spray-melt-quench (SMQ) approach has been adopted. The densities and concentration of atoms in the simulation box were varied in many different cases to successively generate less-correlated local atomic environments reflecting various atomic configurations.

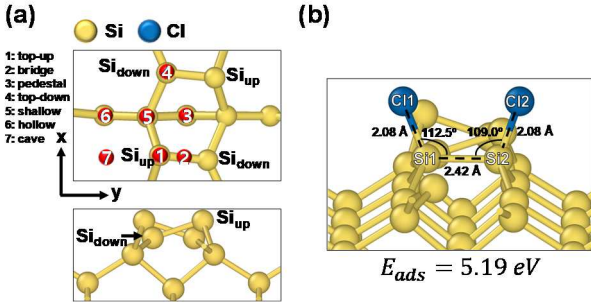


Figure 1: Dissociative adsorption of a chlorine molecule on Si(001) surface. (a) Schematic illustrations of initial positions where a chlorine molecule is introduced. (b) The most probable configuration after dissociative adsorption of a chlorine molecule on the surface.

III. RESULTS AND DISCUSSIONS

A. Dissociative adsorption of a chlorine molecule on Si(001) surface

To investigate the optimized atomic configurations after a chlorine molecule (Cl_2) adsorbed, we considered two geometries and seven surface sites considering high symmetry points for Cl_2 adsorption. The schematics of the sites are depicted in Figure 1(a). Due to the dangling bonds of dimer atoms (Si_{up} and Si_{down}), the chlorine molecule predominantly chemisorbed on the dimer. The adsorption energy which is defined by $E_{ads} = E_{ref} - E$ where E is the total energy of chemisorbed adsorbate on the surface and E_{ref} is the total energy of a reference system (i.e. bare Si(001) slab and isolated Cl_2 molecule) shows 5.19 eV for Si(001) surface which is in good agreement with experimental value [8]. Also the dissociative adsorption reaction was found to be barrierless [5]. Upon the adsorption, the buckled dimer structure in Si(001) has been released which becomes flat structure [9]. The calculated equilibrium parameters are depicted in Figure 1(b). In Figure 1(b), the Cl-adsorbed Si-Si dimer bond length was found to be $\sim 2.42 \text{ \AA}$ which is longer than the pristine dimer bond length (2.37 \AA) and the Si-Cl bond angle was close

Table 1: The valence electron populations corresponding to a Cl_2 adsorption

	Si1 (Si_{up})	Si2 (Si_{down})	Cl1	Cl2
Before Cl_2 ads	-0.07e	0.06e	-	-
After Cl_2 ads	0.29e	0.22e	-0.31e	-0.32e

to the ideal tetrahedral bond angle of 109.5° similar to the experimental results [10]. The longer dimer bond length indicates the weakening of the bond strength associated with charge transfer to the Cl atoms due to the high electronegativity. Voronoi population analysis shows that there is an electron transfer from Si_{down} to Si_{up} atoms about $0.07e$ when the Si(001) surface undergoes its $p(2 \times 2)$ reconstruction [11]. The lone pair accumulated on the Si_{up} serves as the primary access point for the electrophilic attack of a Cl_2 molecule, which the behavior has been expected from the previous ab-initio MD result [5]. After the Cl_2 chemisorption, the dimer atoms contributes $\sim 0.31e$ to each chlorine atom [12]. Table 1 shows the valence electron population corresponding to Cl_2 adsorption. In Figure 2 we plotted the local projected density of states (LPDOS) of the dimer and chlorine atoms. We observed the two chlorine adsorbate (main and subsidiary) peaks separation by $\sim 1.7 \text{ eV}$ as shown in Figure 2(a), which is expected from the low-energy electron energy loss spectroscopy spectra results upon the Cl_2 adsorption on the Si(001) surface [13]. Figure 2(b) shows the LPDOS of the dimer atoms before and after the Cl_2 adsorption. From the plot, we can see that the lowering of the surface states near the valence and conduction band edge upon the Cl_2 adsorption which is related to the passivation of the dangling bonds. Also the appearance of the peak around -4.6 eV has been seen dominantly from the p-orbitals of the dimer atoms [14]. This indicates the strong p-p hybridization between from the adsorbed Cl $p_{x,y}$ -orbital and Si p-orbital as shown in Figure 2(a). It is also in good agreement with the previous results that the transition of Cl(p_z) bonding state to the Cl(p_x, p_y) state, which forms a π -like bonding state [13].

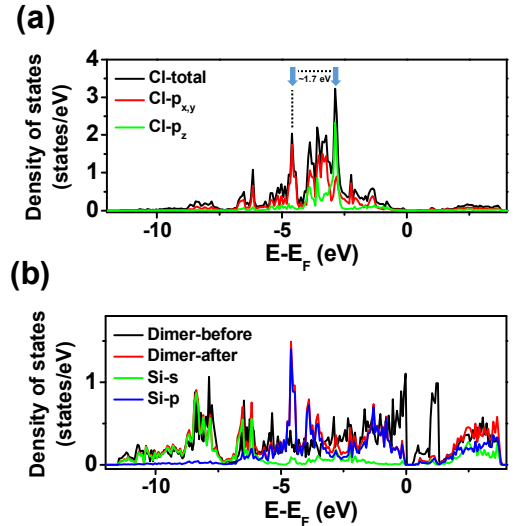


Figure 2: Local projected density of states (LPDOS) projected on the Cl and dimer Si atoms before and after the adsorption.

Table 2: Details of the training set

Structure type	# of structures
Bulk	97
Distorted crystal & Equation of State	
MD (500K)	250
Molecules	
Cl_2	20
0.5, 1ML Cl-terminated Si(001)	200 each
MD, 1000K	
0.5, 1ML Cl-terminated Si(111)	200 each
MD, 1000K	
Spray-Melt-Quench (low density)	40 each
Si:ClH = 1:1:0, 1:1:1, 2:1:0, 2:1:1, 3:1:0, 3:1:1, 4:1:0, 4:1:1, 5:1:0, 5:1:1, 6:1:0, 6:1:1, 8:1:0, 10:1:0, 1:2:0	
Spray-Melt-Quench (medium density)	40 each
Si:ClH = 1:1:0, 1:1:1, 2:1:0, 2:1:1, 3:1:0, 3:1:1, 4:1:0, 4:1:1, 5:1:0, 5:1:1, 6:1:0, 6:1:1, 8:1:0, 10:1:0, 1:2:0	
Spray-Melt-Quench (high density)	40 each
Si:ClH = 1:1:0, 1:1:1, 2:1:0, 2:1:1, 3:1:0, 3:1:1, 4:1:0, 4:1:1, 5:1:0, 5:1:1, 6:1:0, 6:1:1, 8:1:0, 10:1:0, 1:2:0	

B. Surface diffusion and desorption of Cl atoms on Si(001) surface

Chlorine adsorption on the buckled Si(001) surface has been extensively studied in terms of etching pathway and interface structure [9]. When low-energy neutral Cl_2 is used at low temperature (~ 100 K), it is reported that the surface concentration of Cl on Si(001) is about one Cl atom per Si atom (i.e. 1 monolayer; 1ML) at the saturation coverage [15], [16]. However, various surface interactions such as spontaneous etching reaction (i.e. SiCl_2 desorption with no energetic assist of ion bombardment) [8] and surface diffusion of monochlorinated Si bond or Cl atom may affect the resultant interface structure at equilibrium depending on various parameters, including the temperature and Cl coverage [17]. Here, we developed a high dimensional BP type NNP to investigate the atomistic configuration under the influence of temperature at an enlarged length scale (~ 1100 atoms) and a longer time scale (~ 2 ns) with improved accuracy.

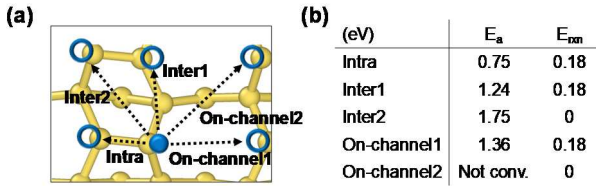


Figure 3: (a) Possible surface diffusion pathways for Cl adatom. (b) Corresponding reaction (E_{rxn}) and activation (E_a) energies for the diffusion pathways.

While developing such NNP, one of major bottleneck of wide applications of the NNP is poor transferability especially when the training set domain covers only limited local environment space for the simulation. To train our NNP for the investigation, ~ 4000 atomic configurations were used. Particularly, we assumed that the most crucial reactions that determines the resultant surface structure at equilibrium would be the 1) Cl adatom diffusion to the first nearest dangling bond on the adjacent dimer atom and 2) spontaneous etching reaction that incorporates twofold coordinated dimer atom diffusion and subsequent desorption of SiCl_2 [8]. Similar desorption mechanism has been proposed for Si(111) surfaces [18]. Besides the reactions, basic configurations such as bulk, slab, and molecule would be included in the training set. Most importantly, so called SMQ approach has been adopted for training set generation. The SMQ method applies typical melt-quench approach which is frequently utilized to generate amorphous structures. By “melting” and “quenching” of a certain simulation box, guided random configurations of the atomic environment can be produced. Since in our case, the local atomic environment reflecting the Si-Cl surface

configuration is important, therefore, we differentiated the density of the simulation box less than the bulk Si density to induce the formation of the Si clusters successfully containing various bulk and surface configurations. Details of the training set is listed in Table 2.

Diffusion of Cl adatom on the Si(001) surface can occur across different diffusion paths as depicted in Figure 3(a). The corresponding reaction and activation energies are depicted in Figure 3(b). Here, only a single Cl adatom has been introduced for the simplified analysis. Depending on the destination of the diffusing Cl atom, the pathway can be classified as intra-dimer (from Si_{up} to Si_{down} in the same dimer), inter-dimer (from Si_{up} to adjacent Si_{up} or Si_{down} in the same dimer row), and on-channel (from Si_{up} to adjacent Si_{up} or Si_{down} across the channel) diffusions. As shown in Figure 3(b), it can be noted that the activation energies generally represent the positive correlation with the hopping distance in case of intra- and inter-dimer diffusions similar to a fluorine diffusion case [19]. In case of the on-channel diffusion, while the straight-line diffusion to adjacent Si_{down} atom across the channel indicated the activation energy of 1.36 eV, diagonal-line diffusion to adjacent Si_{up} atom across the channel failed to converge which is presumably the indication of two-step process involving intermediate states and breakdown of the dimer bond [19]. For training the NNP, we considered each diffusion process by inserting the intermediate images from the cNEB calculations as the components of the training set.

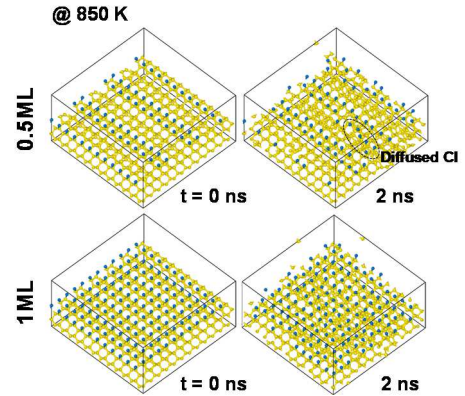


Figure 4: Molecular dynamics (MD) simulations for 0.5ML and 1ML Si(001) surfaces at 850 K for 2 ns.

Using the developed NNP, we conducted MD simulations to study the evolution of the Cl-covered Si(001) surfaces at higher temperature (~ 850 K). We considered 1ML and 0.5ML Cl-covered Si(001) surfaces. To search the most probable Cl configurations for 0.5ML case, five different configurations were investigated. From the figure, it is found that the Cl-covered surface is the most stable when the Cl adatoms gather together while fully passivating each dimer which is in good agreement with previous theoretical results [20]. Figure 4 shows the MD simulations results for the 1ML and 0.5ML Cl-covered Si(001) surfaces at 850 K. For 1ML case, we barely could see any spontaneous desorption of SiCl_2 or surface diffusion of Cl atoms in our simulation time range which is controversial to the experimental results [16]. This is possibly because the surface diffusions are prohibited due to the full saturation of the dangling bonds while the spontaneous desorption reaction shows a higher activation energy (~ 2.4 eV) [8]. Presumably, this indicates that the refinement of the

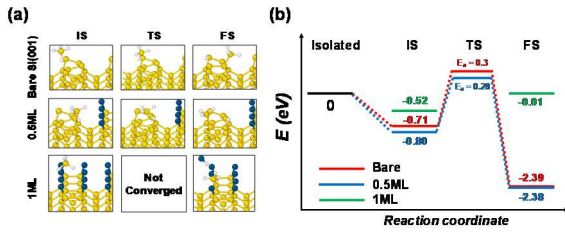


Figure 5: Calculated overall energy diagram of a silane molecule primary adsorption for bare, 0.5ML, and 1ML Si(001) surface. Schematics in (a) show initial and final states of the reaction.

potential is required by searching another spontaneous desorption mechanism and add to the training set to properly reproduce the expected surface characteristics of the Cl surface coverage. Nevertheless, surface diffusion of Cl adatoms indeed has been seen in case of 0.5ML.

C. Adsorption of a silane molecule on Si(001) surface

To understand potential energy landscapes for primary adsorption reactions of silane (SiH_4) chemistry on chlorinated Si(001) surfaces, we optimized the adsorption structures considering two molecular orientations and seven sites for bare Si(001) surface, fourteen sites for 0.5ML Si(001) surface, and six sites for 1ML Si(001) surface. Due to the undercoordinated dimer atoms with the dangling bonds, the SiH_4 molecule predominantly chemisorbed on the dimer similar to the Cl_2 adsorption case. The E_{ads} for the bare and 0.5ML Si(001) surfaces were found to be ~ 2.39 and 2.38 eV, respectively, which is in good agreement with the previous results [21]. Even though there is some portion of dimer atoms that were passivated by Cl for 0.5ML cases, it has no definite effect on the dissociative adsorption of SiH_4 . Also similar tendency can be obtained from the activation energies from cNEB calculations as shown Figure 5(b). The corresponding schematic images of the initial state (IS), transition state (TS), and final state (FS) can be seen in Figure 5(a).

For 1ML Cl-covered Si(001) surface, however, the energetics exhibits quite different properties. Here, the considered adsorption reaction is as following:



where $\text{Si}||$ indicates the surface Si atom. The dissociative reaction is energetically unfavorable as shown in Figure 5(b). Also it is not converged well for the cNEB calculations which may be related to the incorporation of intermediate states in reaction (1) or another reaction mechanism. However, we expect that the activation energy for the reaction would exhibit higher value than the dissociative reaction for the bare Si(001) case based on Bell–Evans–Polanyi principle.

IV. CONCLUSIONS

In summary, we conducted DFT simulations to investigate the impact of surface halogenation on the dissociative adsorption of SiH_4 on crystalline Si(001) surface. First, we examined the adsorption energetics of surface halogenation

using chlorine molecules. The dissociative adsorption of Cl_2 exhibited a high reactivity with the undercoordinated surfaces without barrier. Electronic state analysis revealed the characteristics of monochlorinated Si dimer bond formation. MD simulations using NNP has been developed and adopted to study surface diffusion of adsorbed Cl atoms and the surface concentration of Cl on the Si(001) surface at higher temperature which is affected by spontaneous etching. Second, we conducted subsequent SiH_4 adsorption and the primary hydrogen dissociation on the bare and Cl-passivated surfaces. Our potential energy surface search revealed that the surface halogenation on the silicon surface suppresses the primary adsorption reaction of SiH_4 . Overall, this study provides an atomistic description of the dissociative adsorption mechanisms and associated energies of Cl_2 and subsequent SiH_4 reactions for modeling the epitaxial deposition process and may serve as foundational knowledge for developing next-generation Si epitaxy techniques.

REFERENCES

- [1] R. Reif, A. Fan, K.-N. Chen, and S. Das, "Fabrication technologies for three-dimensional integrated circuits," in *Proceedings International Symposium on Quality Electronic Design*, Mar. 2002, pp. 33–37. doi: 10.1109/ISQED.2002.996687.
- [2] H. Jeong, B. Kim, T. Park, S. Yoo, and S. K. Nam, "Combined molecular dynamics simulations and reaction kinetics study on wettability of trimethylsilyl functionalized silicon surfaces," *Surfaces and Interfaces*, vol. 35, p. 102463, Dec. 2022. doi: 10.1016/j.surf.2022.102463.
- [3] B. Kim, M. Kim, S. Yoo, and S. K. Nam, "Atomistic insights on hydrogen plasma treatment for stabilizing High-k/Si interface," *Applied Surface Science*, vol. 593, p. 153297, Aug. 2022. doi: 10.1016/j.apsusc.2022.153297.
- [4] S. Kim *et al.*, "Atomistic kinetic Monte Carlo simulation on atomic layer deposition of TiN thin film," *Computational Materials Science*, vol. 213, p. 111620, Oct. 2022. doi: 10.1016/j.commatsci.2022.111620.
- [5] H. Okada, K. Inagaki, H. Goto, K. Endo, K. Hirose, and Y. Mori, "First-principles molecular-dynamics calculations and STM observations of dissociative adsorption of Cl_2 and F_2 on Si(001) surface," *Surface Science*, vol. 515, no. 2, pp. 287–295, Sep. 2002. doi: 10.1016/S0039-6028(02)01776-4.
- [6] G. Henkelman, B. P. Uberuaga, and H. Jónsson, "A climbing image nudged elastic band method for finding saddle points and minimum energy paths," *The Journal of Chemical Physics*, vol. 113, no. 22, pp. 9901–9904, Dec. 2000. doi: 10.1063/1.1329672.
- [7] K. Lee, D. Yoo, W. Jeong, and S. Han, "SIMPLE-NN: An efficient package for training and executing neural-network interatomic potentials," *Computer Physics Communications*, vol. 242, pp. 95–103, Sep. 2019. doi: 10.1016/j.cpc.2019.04.014.
- [8] G. A. de Wijs, A. De Vita, and A. Selloni, "Mechanism for SiCl_2 Formation and Desorption and the Growth of Pits in the Etching of Si(100) with Chlorine," *Phys. Rev. Lett.*, vol. 78, no. 25, pp. 4877–4880, Jun. 1997. doi: 10.1103/PhysRevLett.78.4877.
- [9] T.-W. Pi, S.-F. Tsai, C.-P. Ouyang, J.-F. Wen, and R.-T. Wu, "Adsorption of chlorine on the Si(001)- 2×1 surface," *Surface Science*, vol. 488, no. 3, pp. 387–392, Aug. 2001. doi: 10.1016/S0039-6028(01)01163-3.
- [10] W. C. Simpson and J. A. Yarmoff, "Bonding geometries of F and Cl on Si(100)- 2×1 ," *Surface Science*, vol. 359, no. 1, pp. 135–146, Jul. 1996. doi: 10.1016/0039-6028(96)00373-1.
- [11] C. K. Fink and S. J. Jenkins, "First-principles molecular dynamics of the initial oxidation of Si(001) by ozone," *Phys. Rev. B*, vol. 78, no. 19, p. 195407, Nov. 2008. doi: 10.1103/PhysRevB.78.195407.
- [12] B. I. Craig and P. V. Smith, "Chemisorption of HCl, Cl_2 and F_2 on the Si(100) surface," *Surface Science*, vol. 262, no. 1, pp. 235–244, Feb. 1992. doi: 10.1016/0039-6028(92)90474-K.
- [13] N. Aoto, E. Ikawa, and Y. Kurogi, "Low-energy electron energy loss spectroscopy of Cl adsorbed Si(111), Si(100) and Si(110) surfaces," *Surface Science*, vol. 199, no. 3, pp. 408–420, Jan. 1988. doi: 10.1016/0039-6028(88)90911-9.
- [14] D. Casagrande, G. P. Srivastava, and A. C. Ferraz, "Theoretical calculations for Si(001)- $(2 \times 1)\text{Cl}$," *Surface Science*, vol. 402–404, pp. 653–657, May 1998. doi: 10.1016/S0039-6028(97)00929-1.
- [15] K. Seino, W. G. Schmidt, and F. Bechstedt, "Energetics of Si(001) Surfaces Exposed to Electric Fields and Charge Injection," *Phys. Rev. Lett.*, vol. 93, no. 3, p. 036101, Jul. 2004. doi: 10.1103/PhysRevLett.93.036101.
- [16] Q. Gao, C. C. Cheng, P. J. Chen, W. J. Choyke, and J. T. Yates, "Comparison of Cl_2 and HCl adsorption on Si(100)- (2×1) ," *Thin Solid Films*, vol. 225, no. 1, pp. 140–144, Mar. 1993. doi: 10.1016/0040-6090(93)90143-D.
- [17] G. A. de Wijs, A. De Vita, and A. Selloni, "First-principles study of chlorine adsorption and reactions on Si(100)," *Phys. Rev. B*, vol. 57, no. 16, pp. 10021–10029, Apr. 1998. doi: 10.1103/PhysRevB.57.10021.
- [18] S. Sakurai and T. Nakayama, "Adsorption, diffusion and desorption of Cl atoms on Si(111) surfaces," *Journal of Crystal Growth*, vol. 237–239, pp. 212–216, Apr. 2002. doi: 10.1016/S0022-0248(01)01904-2.
- [19] L. Bouamama, A. Lounis, A. Mokrani, A. Ziane, S. Bouarab, and A. Rhallabi, "Density functional theory study of the SiF molecule adsorption and decomposition on $\text{p}(2 \times 2)$ reconstructed Si(001) surface," *Surface Science*, vol. 697, p. 121602, Jul. 2020. doi: 10.1016/j.susc.2020.121602.
- [20] M. W. Radny and P. V. Smith, "A SLAB-MINDO study of half monolayer and monolayer chemisorption of chlorine on the silicon (001) surface," *Surface Science*, vol. 319, no. 3, pp. 232–242, Nov. 1994. doi: 10.1016/0039-6028(94)90590-8.
- [21] H. Park, E. Yoon, G. D. Lee, and H. J. Kim, "Analysis of surface adsorption kinetics of SiH_4 and Si_2H_6 for deposition of a hydrogenated silicon thin film using intermediate pressure SiH_4 plasmas," *Applied Surface Science*, vol. 496, p. 143728, Dec. 2019. doi: 10.1016/j.apsusc.2019.143728.